

## **MILESTONE DELIVERABLE**

### **Task 2.2: 1 kW Generator Prototype Test Results**

**Date of Completion: 03/20/2015**

#### **PROTECTED RIGHTS NOTICE**

These protected data were produced under agreement no. DE-EE0006400 with the U.S. Department of Energy and may not be published, disseminated, or disclosed to others outside the Government until five (5) years from the date the data were first produced, unless express written authorization is obtained from the recipient. Upon expiration of the period of protection set forth in this Notice, the Government shall have unlimited rights in this data. This Notice shall be marked on any reproduction of this data, in whole or in part.

#### **1. GENERAL DESCRIPTION:**

This document describes the results of the experimental performance evaluation of the pole-modulated, 300 rpm generator prototype as well as a tooth wound stator using the same surface permanent magnet outer rotor. The primary goals of these tests are to

- Demonstrate the feasibility of the novel rotor design
- Compare the mass and volumetric torque density of the prototype against the baseline targets
- Measure test data for calibration and validation of performance calculations
- Identify potential risks and opportunities to improve the electromagnetic, mechanical, structural, or thermal performance of the larger second prototype

Following an initial description of the test-set-up and generator configurations, the rest of the report compares mechanical, electromagnetic, and thermal measured test data to finite element calculated predictions.

Finally, a comparison is made between the two configurations of the Phase I prototype and the baseline reference values.

#### **2. TEST SET UP:**

After some initial load tests driving the generator rotor directly using the 20 hp motor where the generator is face-mounted, the test set-up was reconfigured in order to add an in-line torque transducer. A DC drive dynamometer which can provide direct torque measurements of the shaft is utilized for the remainder of the prototype testing. A bare shaft has been substituted in place of the rotor inside the 20 hp induction machine. The same 20hp induction motor frame and bearings are used to support the prototype generators under test. The general layout of the test set-up is shown in Figure 1.

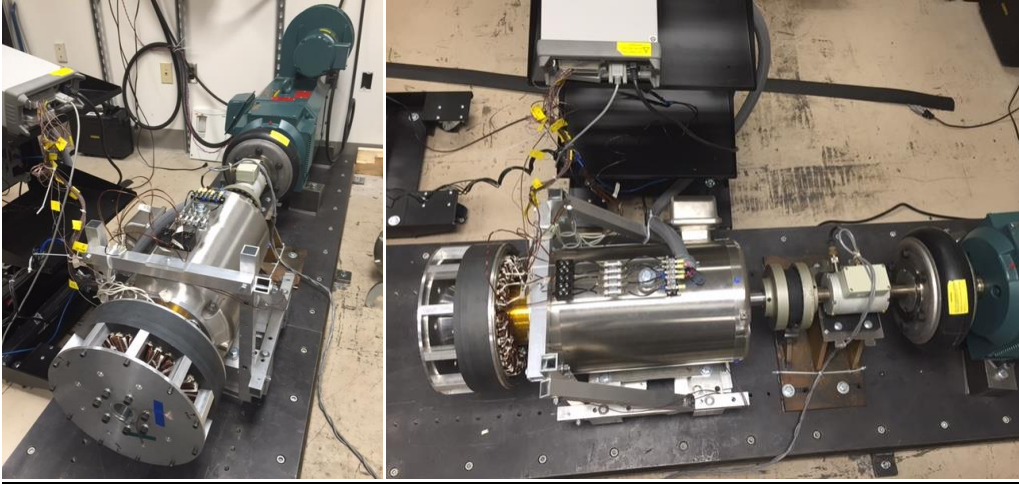
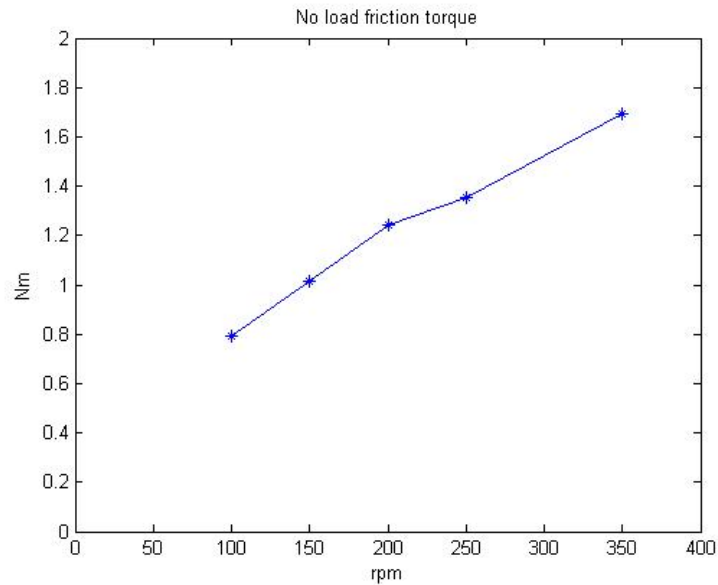


**Figure 1. Reconfigured test set-up**

**Table 1. Dyno components**

| Tooth Wound Prototype | AC Induction Machine | Torque Meter      | DC Drive Machine  |
|-----------------------|----------------------|-------------------|-------------------|
| 4 KW / 300 rpm        | as frame/shaft only  | 400Nm / 8,500 rpm | 45 KW / 4,000 rpm |

For this setup, the generator torque can be directly measured with the face-mounted AC induction machine frame. The dragging torque / power characteristics are provided in Figure 2.



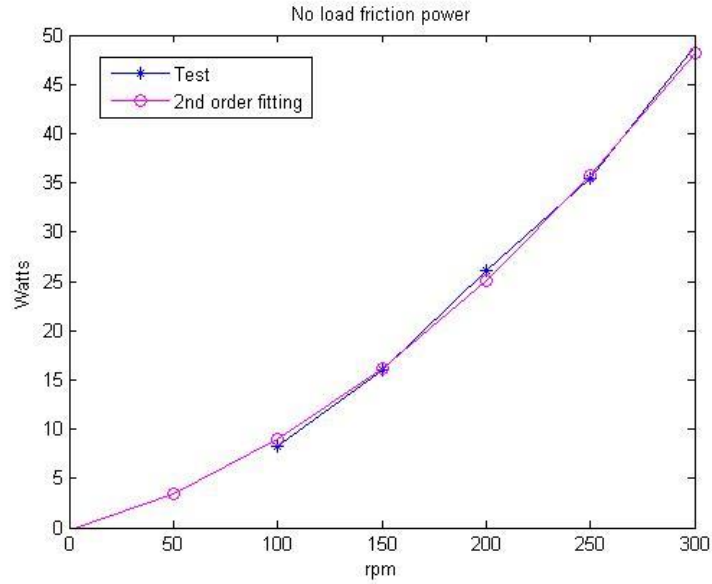


**Figure 2. Dyno shaft torque at no load**

### **3. PROTOTYPE CONFIGURATIONS**

The pole modulated and tooth wound prototype concepts are shown below in Figure 3 and Figure 4.

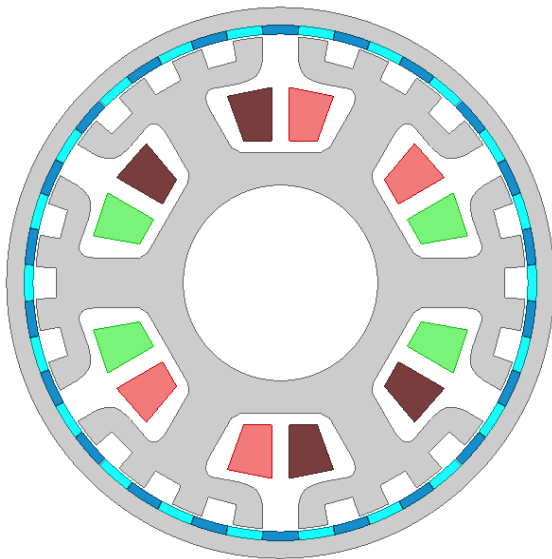


**Figure 3. Pole modulated stator generator configuration**

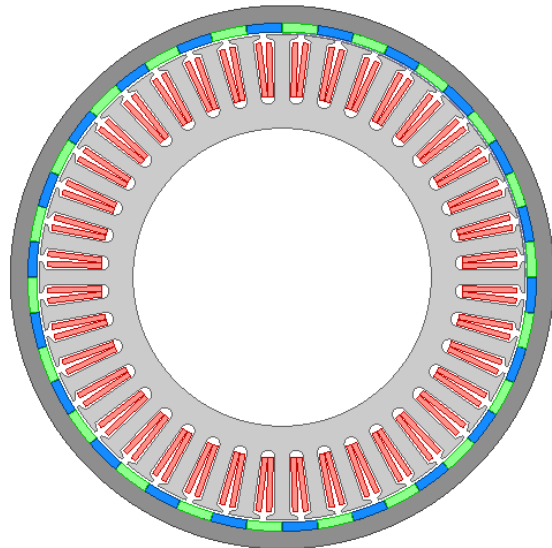


**Figure 4. Tooth wound stator generator configuration**

**Table 2. 300 rpm pole modulated generator characteristics**

|               |     |                |       |
|---------------|-----|----------------|-------|
| Rotor OD (mm) | 310 | Stator OD (mm) | 277.3 |
|---------------|-----|----------------|-------|

|                        |     |                     |      |
|------------------------|-----|---------------------|------|
| Stack Length(mm)       | 60  | Rotor pole number   | 44   |
| Phase number           | 3   | PM thickness(mm)    | 5    |
| PM width (mm)          | 19  | PM length (mm)      | 60   |
| Winding type           | Y   | Turns/Coil          | 75   |
| Modulation Poles       | 48  | Air gap (mm)        | 1.5  |
| PM weight (kg)         | 1.8 | Lam weight (kg)     | 17.2 |
| Raw Active Material \$ | 290 | Winding weight (kg) | 2.4  |

**Table 3. 300 rpm tooth wound generator characteristics**

|                        |      |                     |       |
|------------------------|------|---------------------|-------|
| Rotor OD (mm)          | 310  | Stator OD (mm)      | 277.3 |
| Stack Length(mm)       | 60   | Rotor pole number   | 44    |
| Phase number           | 5    | PM thickness(mm)    | 5     |
| PM width (mm)          | 19   | PM length (mm)      | 60    |
| Winding type           | Star | Turns/Coil          | 48    |
| Stator slot #          | 40   | Air gap (mm)        | 1.5   |
| PM weight (kg)         | 1.8  | Lam weight (kg)     | 15.1  |
| Raw Active Material \$ | 276  | Winding weight (kg) | 2.1   |

#### 4. MECHANICAL CHECK AND FREQUENCY RESPONSE:

First, the rotor runout was checked by partially mounting the rotor on the drive machine, leaving space so that a plunger style deflection gauge attached to a magnetic base could be placed on the interior of the rotor. The rotor was engaged on the shaft roughly one shaft diameter (1.375") and then rotated by hand. The rotor eccentricity was measured to be 0.008", or about 10% of the air gap diameter.

Next, modal modeling and frequency response testing have been performed to examine the prototype rotor resonant frequencies. Finite element analysis on the rotating components of the prototype generator, as well as the supporting shaft and bearing structures were validated by experimentally measuring impulse response data for the rotating components of the Phase I prototype using a small, three-axis accelerometer. Figure 5 shows the ANSYS model of the rotating components. The accelerometer placement is shown in Figure 6. A comparison between the calculated and measured modal frequencies is given in Figure 7. The two major modes occur at about 62 and 112 Hz. The mode frequencies were modeled within 7% of experimental data. The calculated amplitude values are arbitrary and should be disregarded since no attempt was made to measure the impulse force or calculate the vibration amplitudes. No vibration issues are expected during generator testing since no modes are close to the operating range up to 300 rpm, or 5 Hz. Calculated mechanical air gap deflections, too small to measure in the Phase I prototype case, can also be applied to the larger generator designs.

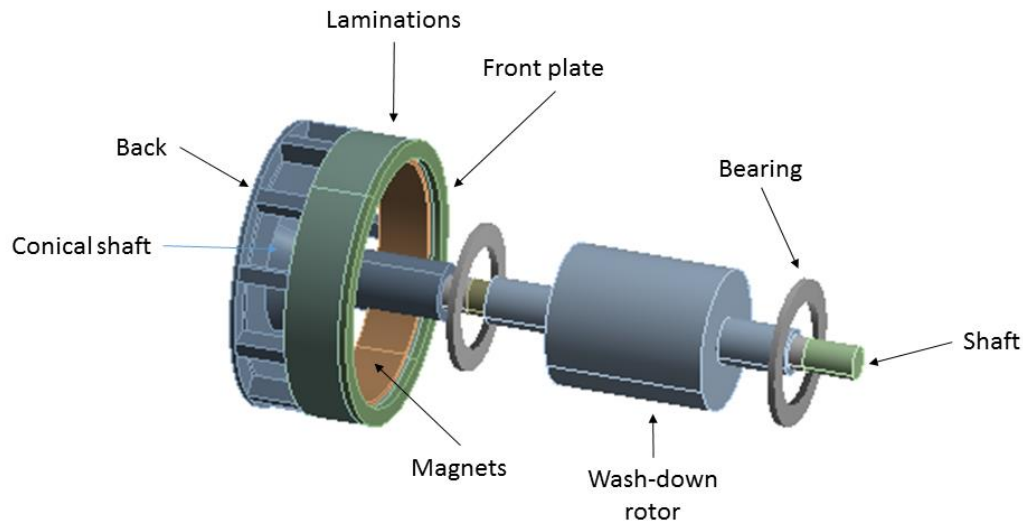


**Figure 5. ANSYS model for the generator rotor and supporting induction motor rotor, shaft, and bearings**

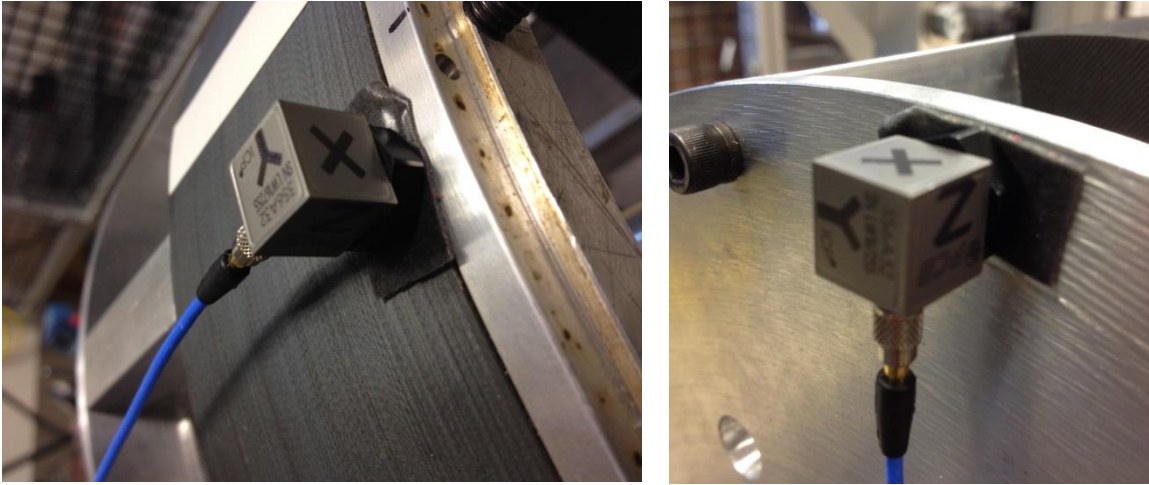


**Figure 6. Accelerometer locations**

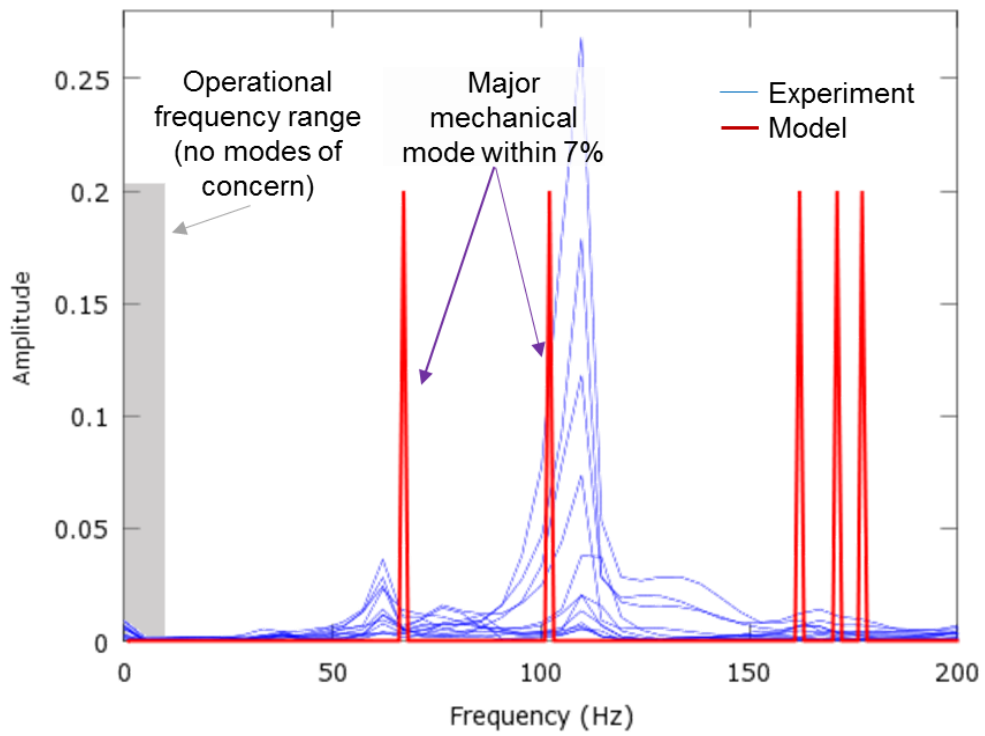


**Figure 7. Comparison of modal modeling and test data**

## 5. Back EMF: Measurement vs Calculation

The open circuit line to line voltage waveforms at 300 RPM for the pole-modulated prototype are overlaid with FEA simulation data as shown in Figure 8. The harmonic component peak values from fundamental up to 30<sup>th</sup> are insignificant, as shown on the right.

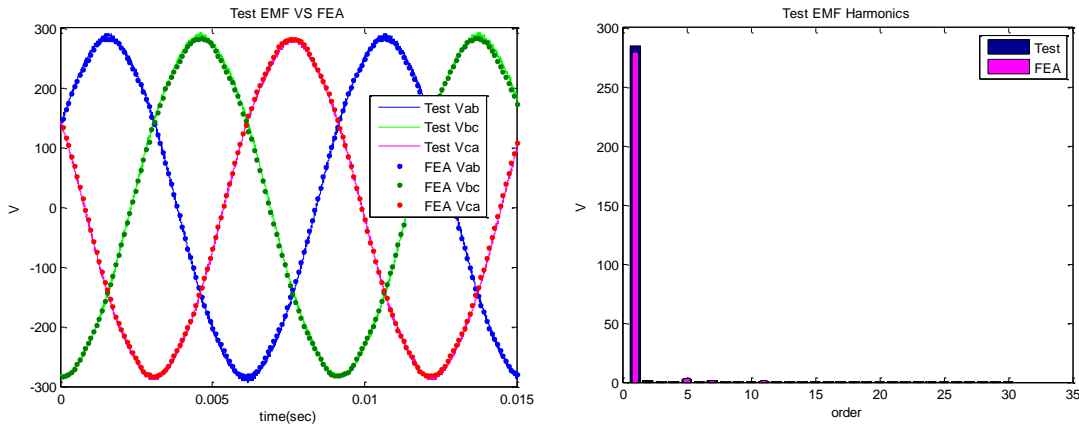


**Figure 8. Pole-modulated stator open circuit back EMF waveforms**

The details of the waveforms are summarized in the table below.

**Table 4. Pole-modulated stator open circuit back EMF waveform characteristics**

| Back EMF Test | Fundamental (V) | THD   |
|---------------|-----------------|-------|
| Test          | 284.5           | 0.88% |
| FEA           | 280.0           | 1.07% |
| Error         | 1.6%            | -     |

Similarly, with phase windings disconnected from the load bank, the prototype tooth wound stator was also tested under no load condition. The measured EMF waveforms are overlaid with FEA simulation data as shown in Figure 9. The harmonic component peak values from fundamental up to 30<sup>th</sup> are include at the right side for detailed comparison.

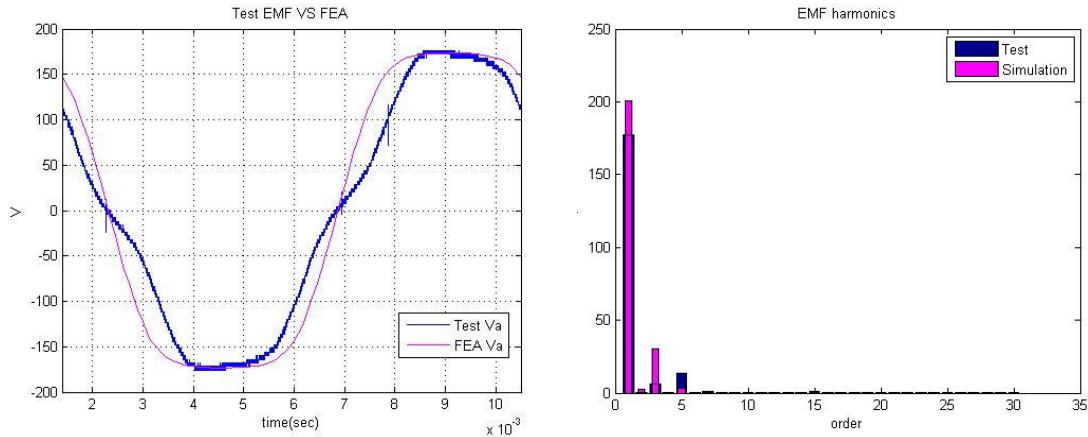


**Figure 9. Tooth-wound stator open circuit back EMF waveforms**

The details of the waveforms are summarized in the table below.

**Table 5. Tooth-wound stator open circuit back EMF waveform characteristics**

| NL Test | Fundamental (V) | THD   |
|---------|-----------------|-------|
| Test    | 177             | 8.4%  |
| FEA     | 200             | 15.3% |
| Error   | 13%             |       |

## 6. POLE MODULATED RESISTIVE LOAD TESTING:

The pole modulated generator has been tested at 1kW while feeding a resistive load. In Figure 10 the load voltage and current are illustrated, with a comparison of measured and predicted power, losses, efficiency and torque density listed in Table 6.

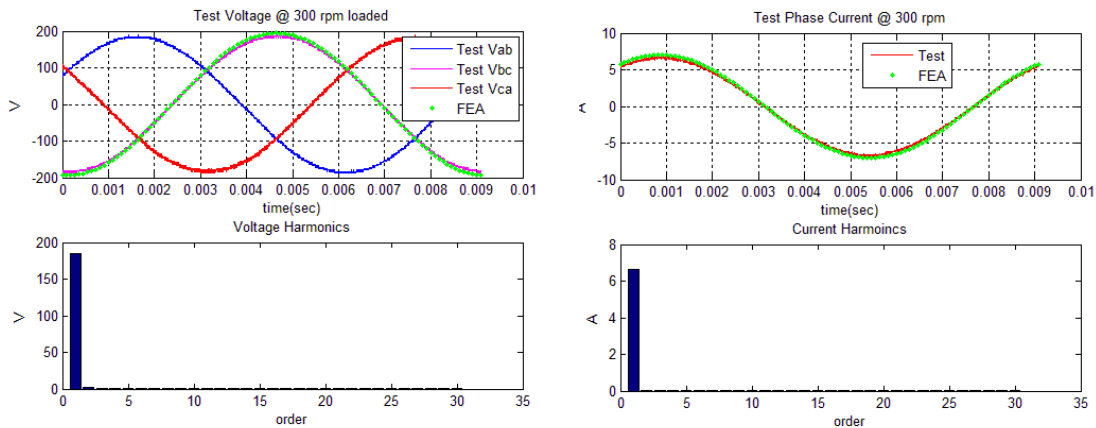


**Figure 10. 1kW resistive load voltage and current comparison**



**Table 6. 1kW resistive load design and test data comparison (300 rpm)**

|        | Power (KW) | Voltage (V,rms) | Current (A,rms) | Total Loss (W) | Effi (%) | Temp Rise (C deg) |
|--------|------------|-----------------|-----------------|----------------|----------|-------------------|
| Design | 1.0        | 133.5           | 4.9             | 138            | 89.6     | 60                |
| Test   | 1.1        | 131.2           | 4.8             | 85             | 92.7     | 15                |
| Error  | -          | 1.8%            | 2%              | -              | -        | -                 |

It should be noted that the pole modulated prototype losses are significantly reduced compared to the original design estimations because of two major design changes during the final design/manufacturing phase: 1) thinner laminations were applied (0.25mm instead of 0.5mm in thickness) for iron loss reduction. 2) The winding configuration was adjusted to achieve as low a phase resistance as possible. With these adjustments, the prototype losses are reduced by about 40% if compared with the original design value.

With different load bank configurations, the Pole Modulated prototype is tested under different resistive loads at 300 rpm as shown in Figure 11. There is generally only a small mismatch in the voltage and current at different operating points. However, an

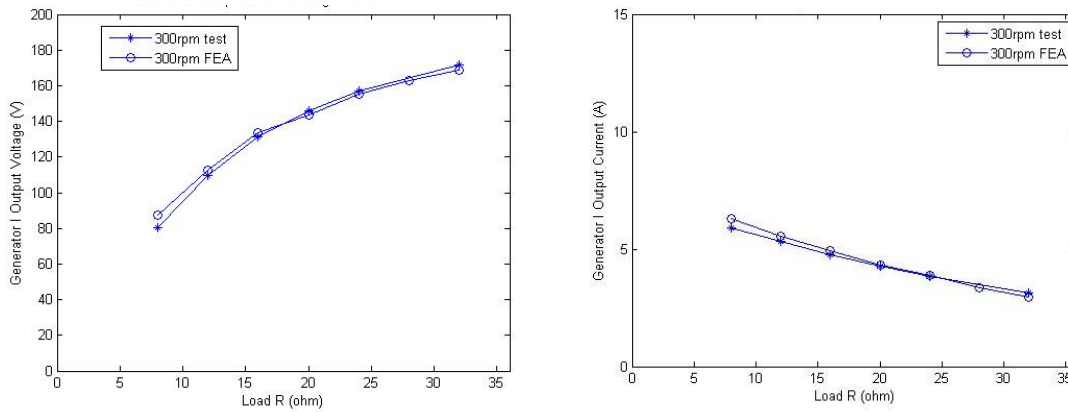


**Figure 11. Pole modulated prototype V/I characteristics with FEA comparisons**

increased difference can be observed as the generator saturates at lower load resistance values and higher load currents, as well as in the power comparisons due to the multiplication of error with the product of voltage and current, as shown in Figure 12.

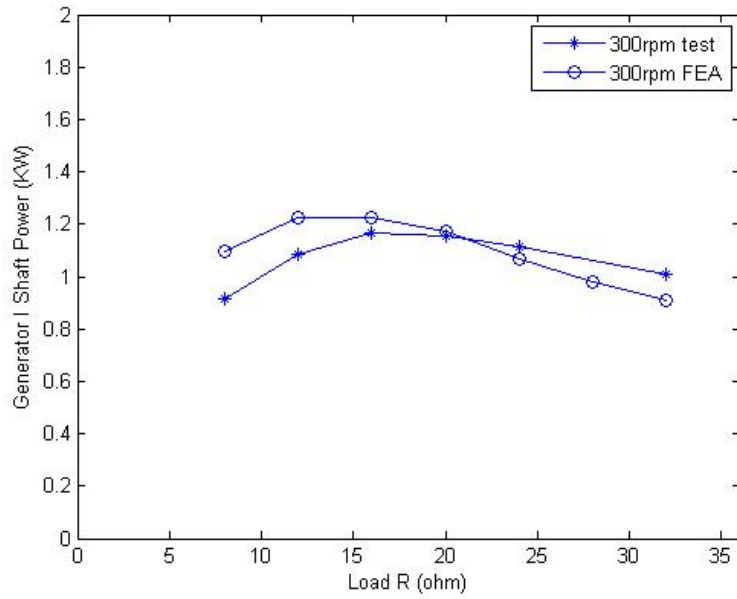


**Figure 12. Pole modulated output power characteristics with FEA comparisons**

At rated 300rpm speed, the pole modulated generator can deliver 1 kW of power over a large range of load resistance, from 10 ohms to over 30 ohms. The breakdown of the generator loss is also investigated with the results plotted in Figure 13.

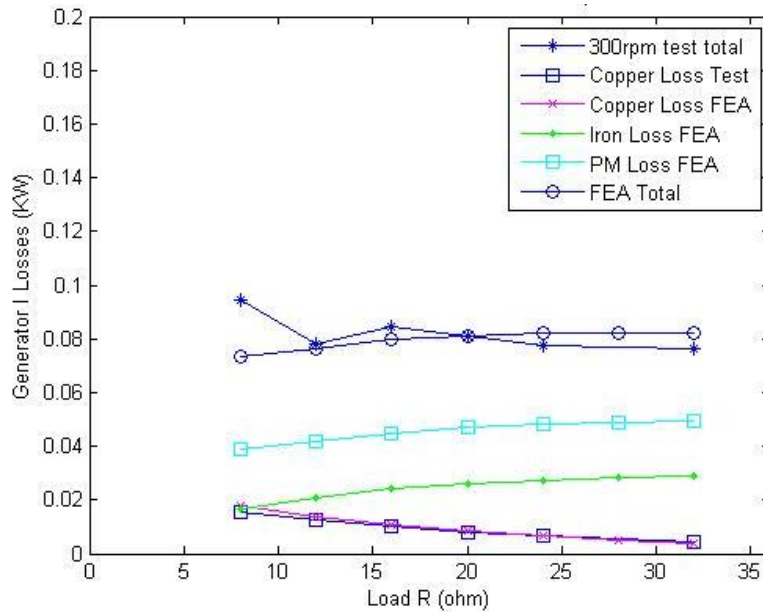


**Figure 13. Pole modulated prototype losses with FEA comparisons**

The pole modulated prototype efficiency is above 90% over a wide resistive load range as indicated in Figure 14, with left plot VS load resistance and right plot VS output power.

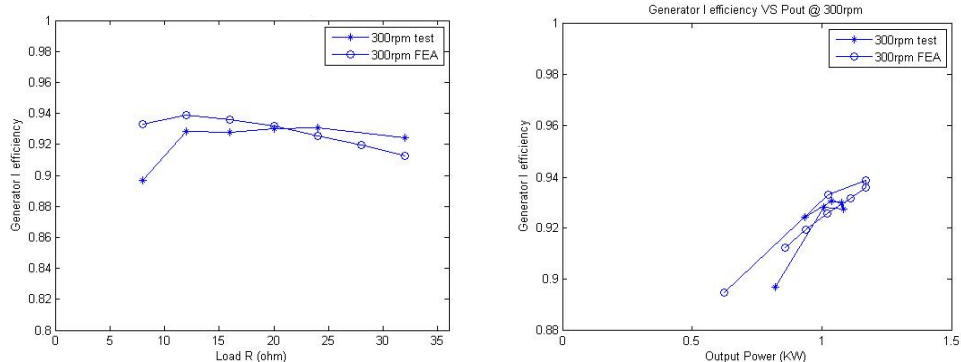


**Figure 14. Pole modulated prototype efficiency with FEA comparisons**

With load power factor adjustment, the pole modulated prototype can be operated in the “over-excited mode” which is expected to deliver significantly higher power and thus higher torque density. With only one prototype rotor built for testing, this over-excited mode is scheduled at the end of the Phase I testing after completing testing of the tooth wound stator.

## **7. POLE MODULATED RESISTIVE-CAPACITIVE LOAD TESTING:**

As predicted in the design phase, the pole modulated generator has higher power output capability when it is operated in the leading power factor domain. With different capacitor bank configurations, the pole modulated prototype is tested under a few different RC loads at 300 rpm and the major characteristics are shown in Figure 15.

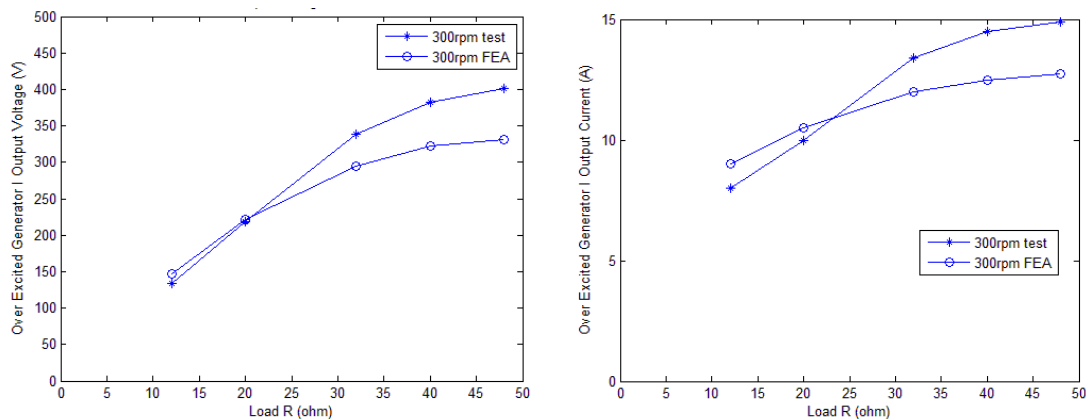


**Figure 15. Pole modulated prototype V / I characteristics with over excitation operation**

With non-constant characteristics of the capacitor bank in different operation domain, there are significant gaps between the simulation results and test data, especially at higher currents. The efficiency characteristics for these operation points are provided in Figure 16.

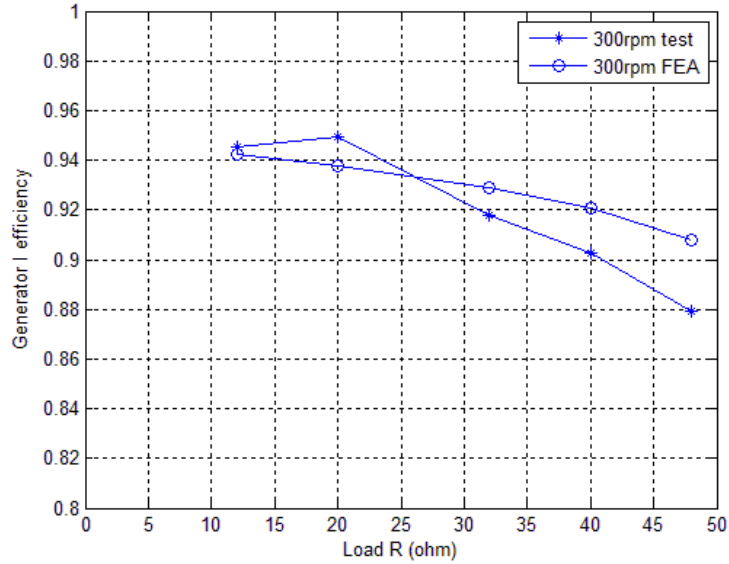


**Figure 16. Pole modulated efficiency characteristics with over excited operation**

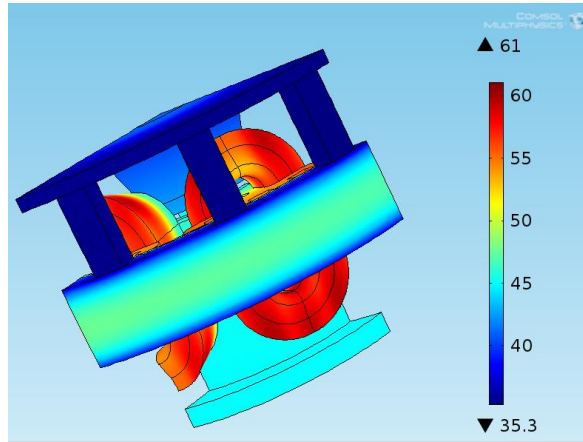
The highest power output observed with the RC load combinations is provided in Table 7.

**Table 7. Pole modulated performance under over excited operation**

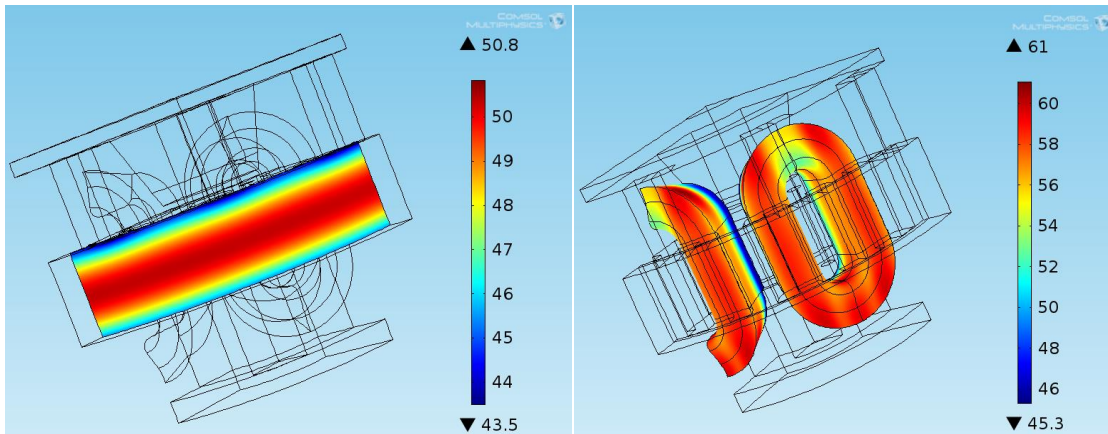
|                       | Power (kW) | Voltage (V) | Current (A) | PF   | Efficiency (%) |
|-----------------------|------------|-------------|-------------|------|----------------|
| Pole Modulated Design | 4.1        | 300         | 12.5        | 0.52 | 92.9           |
| Pole Modulated Test   | 3.7        | 330         | 14.2        | 0.46 | 91.8           |

### **8. POLE MODULATED HEAT RUN:**

The magnet and stator winding temperatures were monitored during all tests, but specific heat runs were also performed using the pole modulated stator operating at about 1.2 kW feeding a resistive load and about 3.65 kW with a resistive-capacitive load. For the lower power case, the generator temperature rise was insignificant, and the drive motor operating at the low speed was a significant source of heat. Both lumped parameter and finite element models were used to predict the motor temperature distribution at about 3.65 kW power output.



(A)



(B)

(C)

**Figure 17. Pole modulated steady state thermal modeling at 3.65 kW**

Results in Figure 12 (3.65 kW) are summarized as below:

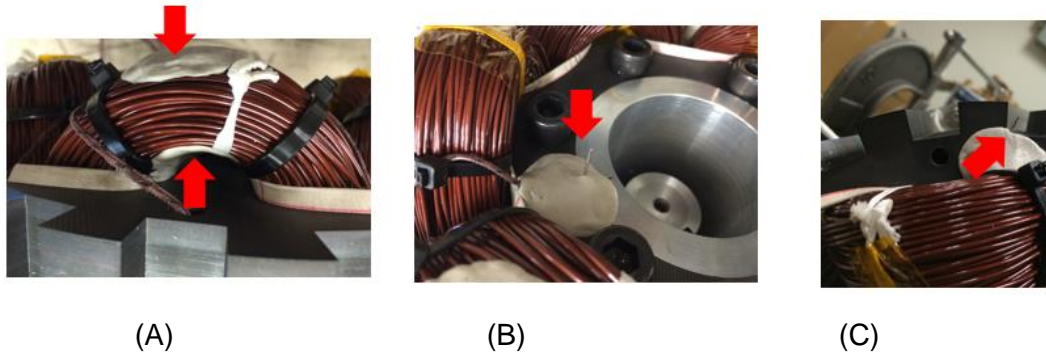
- I. Temperature distribution on different parts of the 3.65 kW generator indicates the highest temperature occurs on the stator windings
- II. The center part is the hottest part of the magnets since the supporting rotor structure components on both sides act as heat sinks
- III. The face mounting surface (20hp stainless steel induction motor) functions as a heat sink, and consequently the parts of the winding which are in contact with stator shaft (stand) show lower temperatures. The highest temperature on the winding is about 60 C on the surface facing to air, and the lowest temperature is about 46 C on the surface facing and connecting to the face-mounting induction motor frame (Fig. 12(C))

Table 8 compares average temperatures as results of steady state lumped parameter and steady state finite element thermal modeling for the 3.65 kW power rated case.

**Table 8. Comparison between average temperatures as the results of LPM and FEM**

| Part                      | Average temperature (degC) |     | $T_{LP} - T_{FE}$ |
|---------------------------|----------------------------|-----|-------------------|
|                           | LPM                        | FEM |                   |
| End winding inside rotor  | 54                         | 56  | -2                |
| Winding inside stator     | 54                         | 56  | -2                |
| End winding outside rotor | 53                         | 56  | -3                |
| Stator back iron          | 51                         | 53  | -1.5              |
| Stator teeth              | 52                         |     |                   |
| PM                        | 46                         | 49  | -3                |
| Rotor back iron           | 42                         | 46  | -4                |

Next, the thermal model results will be compared with measured temperatures during the heat run tests. During the experimental studies, seven J-type wired thermocouples have been installed for measuring the temperatures of the end windings (inside and outside the rotor), on the end plate of the drive motor, inside the drive motor (on the end windings), and facing toward the air (inside and outside the rotor, and toward the air gap). Also one J-type wireless thermocouple has been installed on the rotor end plate where its sensor has been placed between magnets for monitoring the magnets' temperature. Figures 13 and 14 illustrate the positions of some of the thermocouples.



**Figure 18. Wired thermocouples for measuring temperatures, (A) end winding, (B) air inside the rotor, (C) air in the entrance of the air gap**

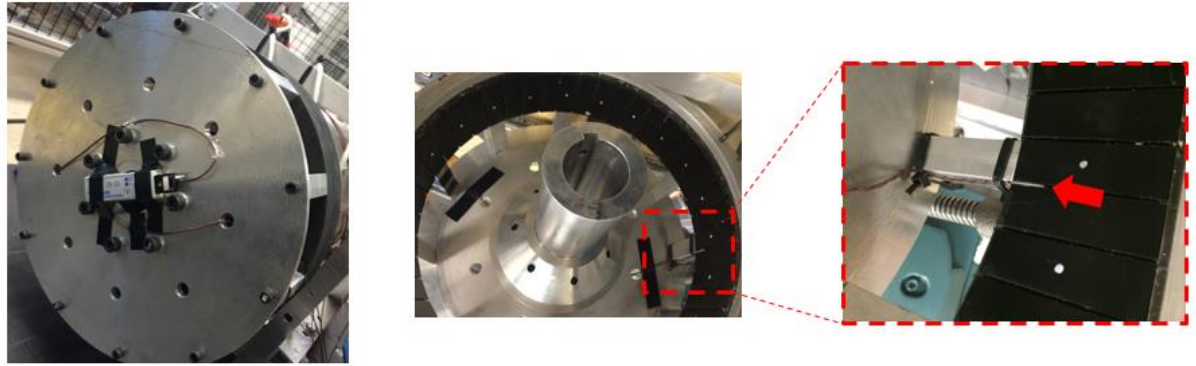


**Figure 19. Wireless thermocouple for measuring magnets' temperature on the rotor**

As comparisons between simulation and measurement show:

- Results of finite element modeling are in good agreement with experimental results (less than 10% difference, and the finite results over estimate the experimental results)
- Difference between numerical simulation and experimental results might be from error in thermocouple reading (thermocouple's surface attachments, rotational motion effect on wireless transmission), error in calculating convection coefficients (lack of precise semi-empirical correlations for the complicated machine geometry), error in calculating thermal losses, or error in calculations of thermal properties of the materials
- Experimental and numerical results showed internal diameter of the end windings are in higher temperatures than outer diameter of the end winding. (These results might be because of weaker convection effect on internal surfaces)
- Highest measured temperature is on the face mounting motor end plate surface

Table 9 presents steady state finite element temperature results versus steady state experimentally measured temperatures for different parts of the pole modulated generator at 3.65 kW.

**Table 9. Steady state FE temperature results versus steady state experimentally measured temperatures for different parts of the 3.65 kW power rated generator**

|                              | Experimental<br>(degC) | FE model<br>(degC) | $T_{exp} - T_{FE}$ |
|------------------------------|------------------------|--------------------|--------------------|
| End winding inside rotor _2  | 53                     | 55                 | -2                 |
| End winding inside rotor _1  | 58                     | 56                 | +2                 |
| End winding outside rotor _2 | 52                     | 57                 | -5                 |
| PM                           | 56                     | 51                 | +5                 |

A prototype pole modulated, exterior rotor permanent magnet machine was thermally studied using steady state lumped parameter analysis (applying SIMULINK/MATLAB software), transient and steady state three dimensional finite element modeling (using

COMSOL software), and experimental examinations using wired and wireless thermocouples. Comparison between transient simulation and experimental thermal results has been carried out. Results of FE modeling were in good agreement with the experimental results. Similar thermal analysis and measurement can be applied to the Phase II design and testing in order to push the temperature limits for the generator design while also maintaining safe operation.

### 9. TOOTH WOUND RESISTIVE LOAD TESTING:

A tooth wound stator has been developed to utilize the same 44 pole, surface PM outer rotor, which allows investigation of another generator topology with reduced engineering design efforts and prototype cost. The tooth wound stator is designed with five phases in order to maximize the winding factor while still using the same 44 pole rotor originally designed for the pole modulated stator. The tooth wound stator can deliver higher power output at unity power factor compared with the pole modulated stator.

Generator performance was measured under a range of resistive loads. In Figure 20, the generator full load voltage and current are illustrated, with the comparison of full load power, losses, and efficiency listed in Table 10.

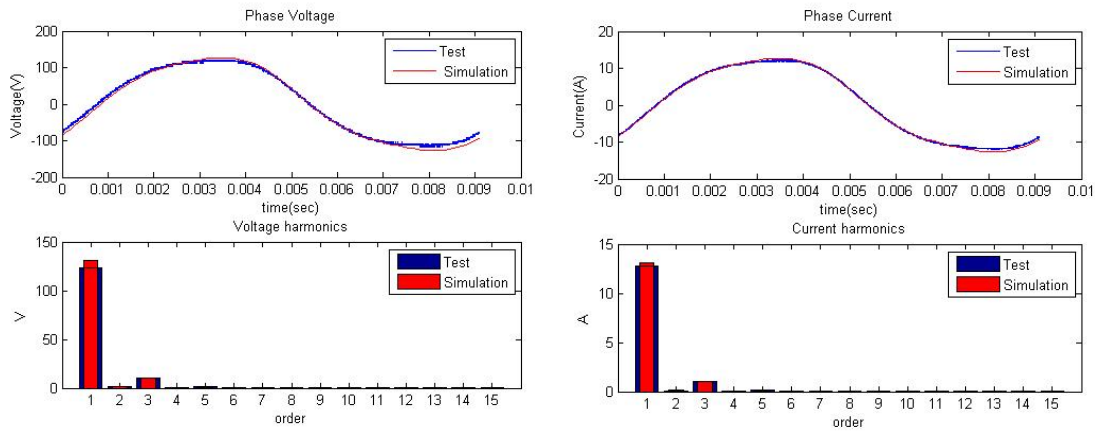


Figure 20. Tooth wound voltage and current waveform comparison

Table 10. Tooth wound design calculations compared to test data

|        | Pout (KW) | Voltage (V,rms) | Current (A,rms) | Total Loss (W) | Effi (%) | Temp Rise (C deg) |
|--------|-----------|-----------------|-----------------|----------------|----------|-------------------|
| Design | 4.0       | 90              | 9               | 396            | 91       | 100               |
| Test   | 4.07      | 89              | 8.9             | 350            | 92.1     | 90                |
| Error  | -         | 1.1%            | 1.1%            | -              | -        | -                 |

It should be noted that the Tooth Wound prototype losses are reduced compared to the original design estimations because thinner laminations were applied (0.25mm instead of 0.5mm in thickness) for iron loss reduction. With this adjustment, the prototype losses are reduced 13% if compared with the calculated values. The direct benefit of loss reduction is that the tooth wound prototype exhibits less than predicted temperature rise. The generator hot spot temperature rise is less than 90 C degree in the 3 hour thermal run without extra cooling method applied in the lab environment.



With different load bank configurations, the tooth wound prototype is tested under different resistive loads as illustrated in Figure 21.

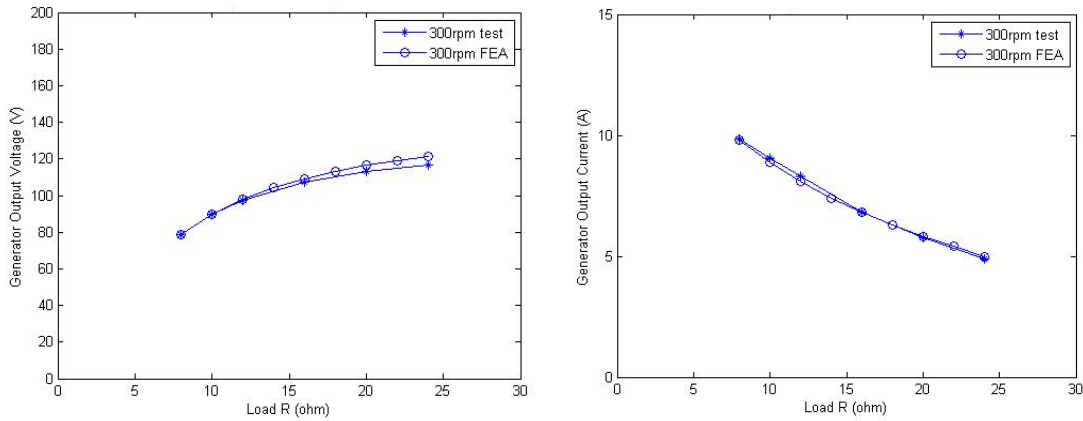


**Figure 21. Tooth wound prototype V / I characteristics with FEA comparison**

With only slightly over-estimated voltage and current at most operating points, the difference is still magnified for the power comparison due to the squaring effect from the product of the voltage and current, as shown in Figure 22.

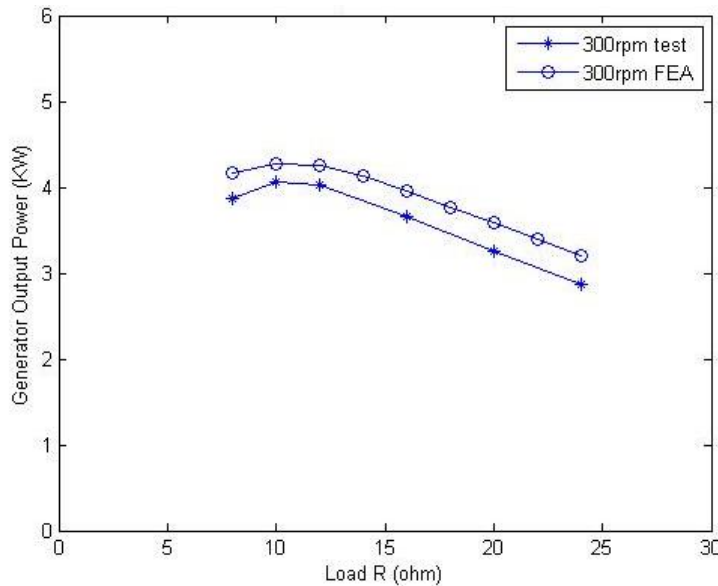


**Figure 22. Tooth wound prototype output power characteristics with FEA comparison**

At rated speed, the generator can deliver 4 kW power output over a range of load resistance from 8 ohms to about 15 ohms. The breakdown of the loss is also investigated with the results plotted in Figure 23.

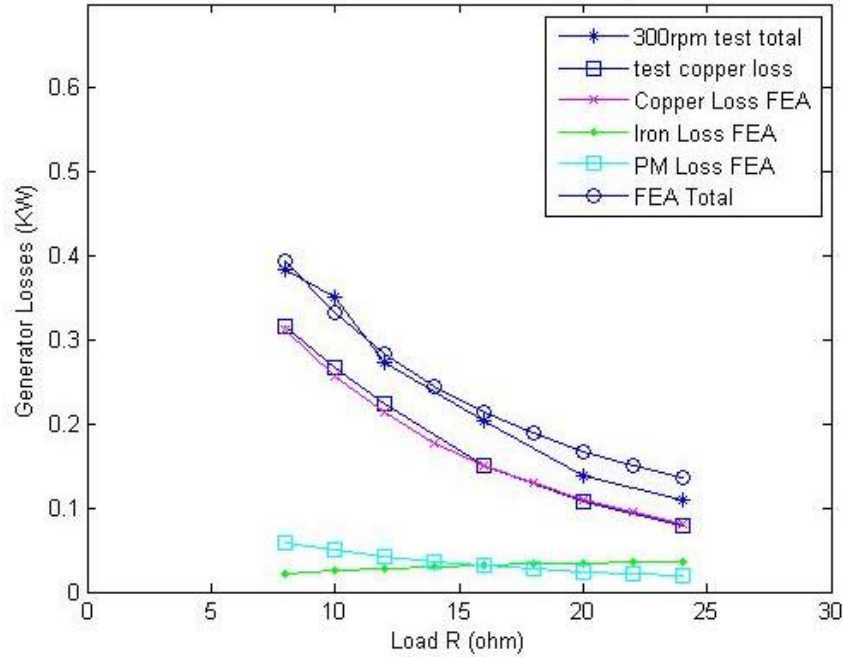


**Figure 23. Tooth wound prototype losses with FEA comparisons**

The tooth wound prototype efficiency is also above 92% for a broad load range as indicated in Figure 24, plotted versus load resistance on the left and versus output power on the right.

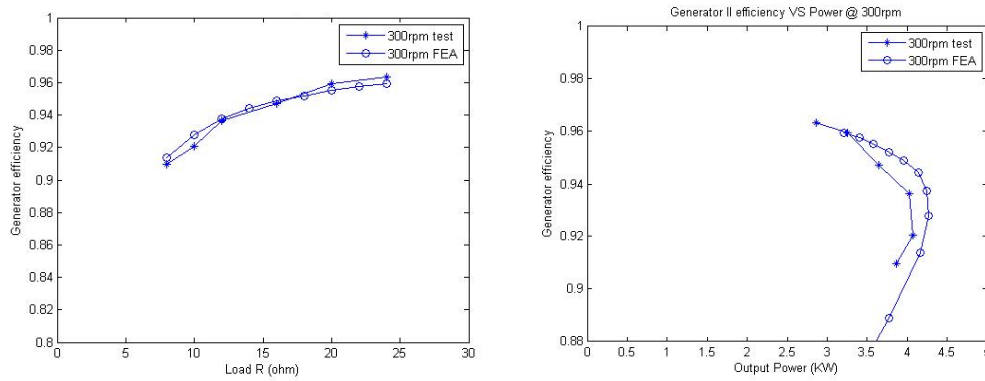


**Figure 24. Tooth wound prototype efficiency with FEA comparisons**

For the targeted wave energy conversion power generation application, the DC link is a required power conversion stage between generator and fixed frequency output electric power feed to the grid. Thus, the power characteristics of the rectified operation are also interesting for the system level investigation, which is performed next.

## **10. TOOTH WOUND DIODE RECTIFIER LOAD TESTING:**

With rectified load bank configurations, the Tooth Wound prototype is tested under different resistive loads and speed as illustrated in Figure 25.

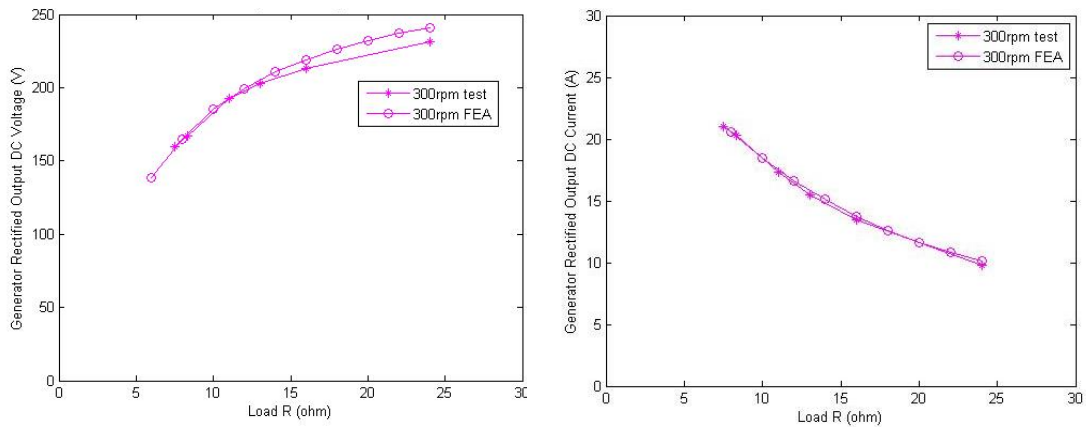


**Figure 25. Tooth wound prototype rectified V / I characteristics with FEA comparison**

Similarly to the AC operation, the machine also observes slightly higher output power if compared with FEA simulations, as shown in Figure 26.

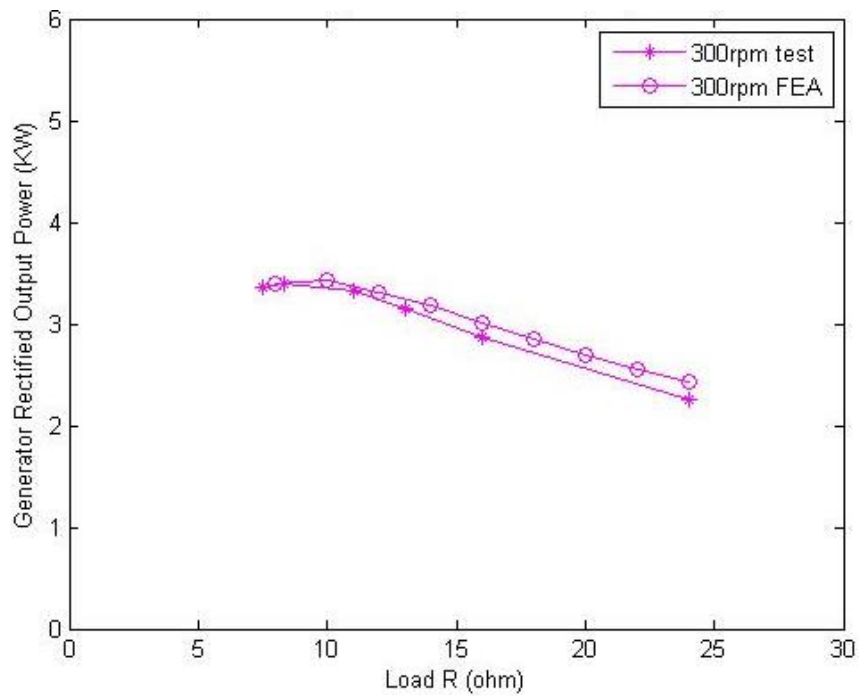


**Figure 26. Tooth wound prototype rectified output power with FEA comparison**

The breakdown of the loss is also investigated with the results plotted in Figure 27.

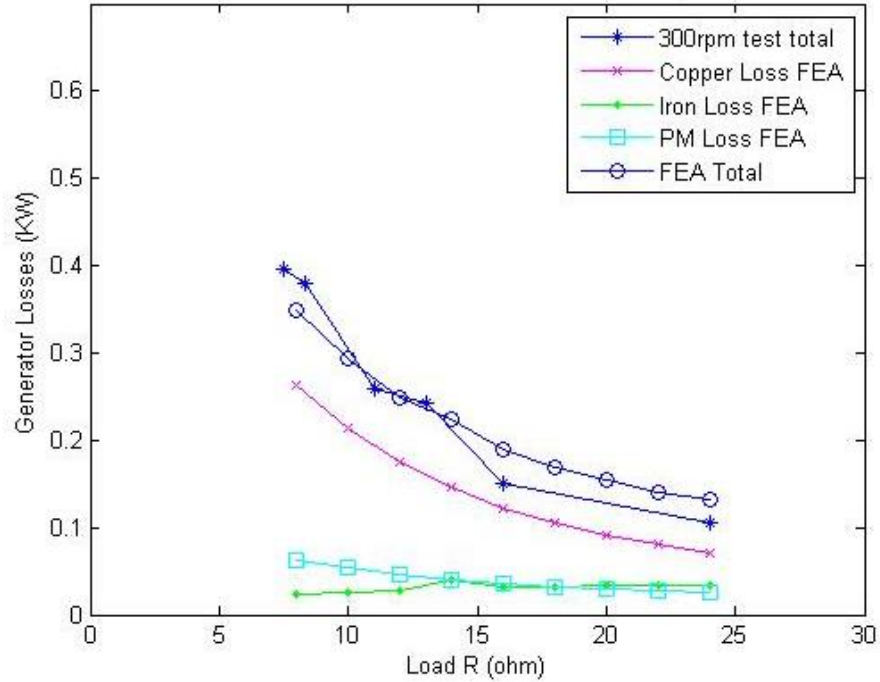


**Figure 27. Tooth wound prototype rectified operation losses with FEA comparison**

The tooth wound prototype efficiency under rectified load is above 90% for a wide load range as indicated in Figure 28.

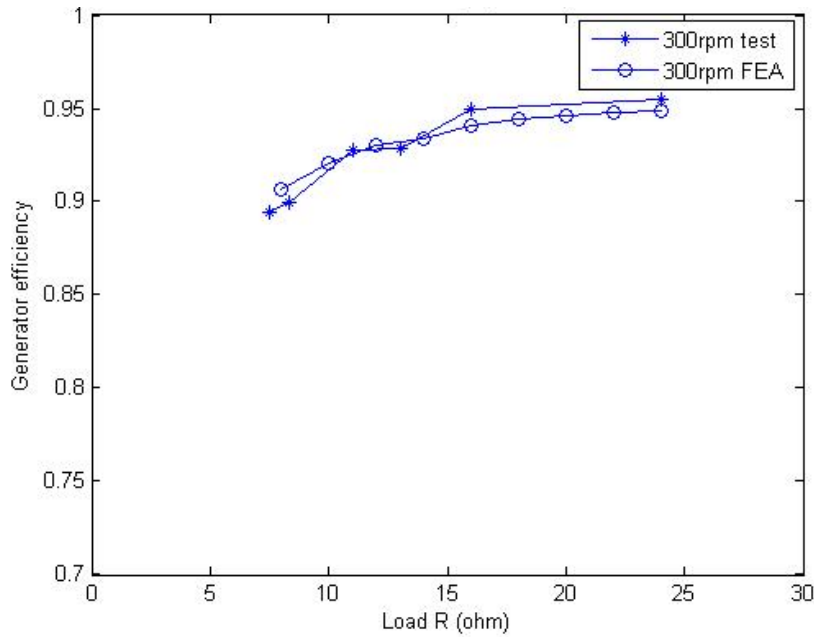


**Figure 28. Tooth wound prototype rectified operation efficiency with FEA comparison**

For comparison, the measured DC bus voltage profile at 300 rpm is plotted versus FEA simulations as shown in Figure 29.

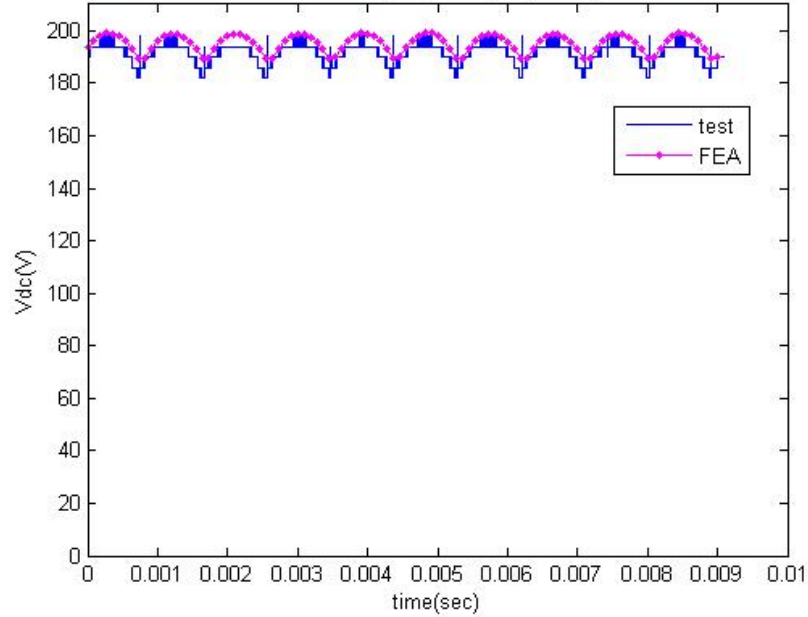


**Figure 29. Tooth wound prototype rectified Vdc with FEA comparison**

## **11. PROTOTYPE TEST COMPARISON, SUMMARY, AND CONCLUSIONS**

In Table 11, the machine major design dimensions, performance index on the shear stress and torque density are provided for comparisons. The torque volume density is evaluated including the length of the the end winding section. The torque weight density is assessed with the active material weight in for these designs.

**Table 11. Generator topology comparison**

|   | Base PM Machine | Pole Modulated                | Tooth Wound  | Target    |
|---|-----------------|-------------------------------|--------------|-----------|
| Machine OD (mm)                             | 310             | 310                           | 310          | -         |
| Air gap OD (mm)                             | 184.2           | 278.8                         | 278.8        | -         |
| Air gap length (mm)                         | 0.89            | 1.5                           | 1.5          | -         |
| Stack length (mm)                           | 152.4           | 60                            | 60           | -         |
| Power (KW)                                  | 5.2             | 1.0 (PF=1)<br>3.8 (PF = 0.5)  | 4.1 (PF=1)   | -         |
| Torque (Nm)                                 | 165.5           | 31.8 (PF=1)<br>121.0 (PF=0.5) | 130.5 (PF=1) | -         |
| Efficiency                                  | 87%             | 92% (PF=1)<br>90% (PF = 0.5)  | 92% (PF = 1) | -         |
| Shear Stress (kN/m <sup>2</sup> )           | 20.5            | 4.3 (PF=1)<br>16.5 (PF=0.5)   | 17.8 (PF=1)  | -         |
| Torque Volume Density (kNm/m <sup>3</sup> ) | 8.2             | 3.4 (PF = 1)<br>13 (PF = 0.5) | 19 (PF = 1)  | <b>16</b> |
| Torque Weight Density (Nm/kg)               | 1.8             | 1.5 (PF=1)<br>5.7 (PF = 0.5)  | 6.9 (PF = 1) | <b>4</b>  |

- 1) Both prototypes have been designed and tested and the results are consistent with the design predictions
- 2) The inline torque transducer was necessary for accurate torque and efficiency measurements.
- 3) The pole modulated design uses the iron pole harmonics in the air gap region. The stator structure is simple and easy to manufacture. It can achieve high power and torque under low, leading power factor operation, which introduces extra loss and cost from the system side for power factor conditioning and higher currents.
- 4) The tooth wound design features a high winding factor which contributes to the target power generation density with the power factor close to unity. While the stator winding coils will be more effort to manufacture than with the pole modulated design, a modular design and machine winding process can be applied to significantly reduce the manufacturing cost.
- 5) The PM loss is not a major loss component as observed in these prototype tests. Large thermal margin and low rotor temperature were observed during tests on both prototypes. The iron and PM losses are not concerns for the targeted low speed application. The stator winding loss is the most significant source of generator loss.